Growth temperature dependence of the magnetic and structural properties of epitaxial Fe layers on MgO(001)

S. M. Jordan, J. F. Lawler, R. Schad, H. van Kempen[a)]
Research Institute for Materials, University of Nijmegen, Toernooiveld 1, NL-6525 ED Nijmegen, The Netherlands.

(Received 10 November 1997; accepted for publication 29 April 1998)

We have studied the growth and magnetic properties of molecular beam epitaxy grown layers of bcc Fe(001) on MgO(001) substrates at a wide range of temperatures. For growth temperatures in the range 80−595 K, the iron forms islands which increase in lateral size with increasing temperature. Completed films in the same temperature range show the magnetic properties expected for a system with biaxial anisotropy, and a coercivity of <10 Oe. The value of the first cubic anisotropy constant divided by the magnetization (K_1/M) remained constant. No evidence for uniaxial magnetic anisotropy in the films was found. Above 595 K, the films' structure and magnetic properties changed dramatically to those characteristic of a particulate system. © *1998 American Institute of Physics.* [S0021-8979(98)06315-4]

I. INTRODUCTION

MgO(001) forms an ideal substrate for the growth of iron layers for several reasons. Firstly, the lattice mismatch is only 4%, and the substrate is robust, transparent and easily obtained in large pieces. A monolayer of Fe on MgO is predicted to display a highly enhanced magnetic moment.[1] A uniaxial magnetic anisotropy in films evaporated at an oblique angle of incidence has also been seen,[2,3] and attributed to in-plane distortion of the Fe. The Fe(001) surface is also expected to display a highly spin-polarized surface state.[4] Interesting points are that the predicted enhanced magnetic moment has not been confirmed experimentally;[5] neither has the spin-polarization of the surface state.

The molecular beam epitaxy (MBE) growth of one material upon another is influenced strongly by surface diffusion, which allows transport of material during the ordering process. Above a critical temperature, the Schwoebel barrier[6] is overcome, and atoms can diffuse not only in an upward but in a downward direction at step edges. Thürmer *et al.*[7] found Fe/MgO to form an ideal Schwoebel system.

Several growth[8–11] and magnetic[12,13] studies of thin epitaxial films have already been reported. This study differs in that we report direct measurements of the surface morphology using scanning tunneling microscopy (STM) over a wide deposition temperature range. We were also able to measure the magnetic properties of samples immediately after their *in situ* STM investigation. In addition, we have used a novel technique to measure the magnetic anisotropy magneto-optically.

II. SAMPLE PREPARATION

Commercial substrates were cleaned by washing first with hexane, then with acetone and finally rinsed twice with propan-2-ol. 50 nm thick Au stripes were deposited on two sides close to the edges of the MgO to provide a reliable electrical contact between the deposited film and the Mo sample holder. The substrates were heated to 1070 K in ultrahigh vacuum (UHV) for 1 minute and then analyzed by Auger electron spectroscopy (AES). A *KLL* C peak was seen corresponding to 6% of 1 monolayer. Heating the MgO to temperatures as high as 1400 K did not reduce this contamination. No traces of Au were found in the center of the sample. Atomic force microscopy investigations showed the substrates to be of exceptional flatness; single atom high terraces of width up to 200 nm were seen.

Fe layers were grown using a Knudsen cell at a rate of 0.13 nm per minute. The iron atoms were incident at angle of 15° to the sample normal, the flux being directed along the Fe[110] axis. The sample was maintained at the required temperature by electron heating of the sample holder; liquid nitrogen cooling was also available.

III. LOW-ENERGY ELECTRON DIFFRACTION (LEED) INVESTIGATION

The completed films were examined by LEED confirming that the Fe[110] axis is parallel to MgO[100], and the (001) planes of the two materials are parallel. Only weak correlation with temperature was found, the diffracted spots becoming less diffuse as the temperature was increased. A sample grown at 80 K was warmed to room temperature during LEED observations. It was observed that the pattern changed in a nontrivial way, some diffracted orders becoming more diffuse with others becoming sharper. This indicates that the film changes in structure as the temperature is increased. The samples grown below room temperature should be considered as annealed samples, since the STM and magneto-optic Kerr effect (MOKE) studies were carried out at room temperature.

IV. STM INVESTIGATION

STM investigations of the samples were made *in situ* using a locally developed STM. Representative images of 5

a)Corresponding author, Electronic mail: hvk@sci.kun.nl

 © 1998 American Institute of Physics

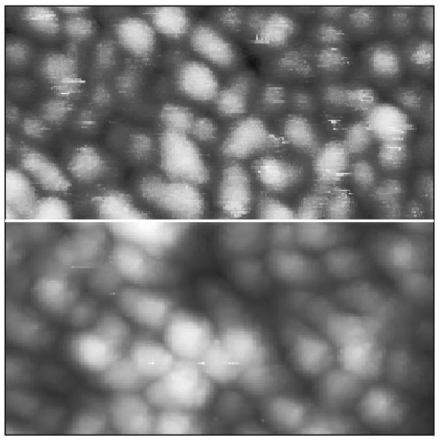

FIG. 1. STM images for growth at 80 (top) and 295 K (bottom). Image sizes 50×25 nm. Black-white contrast is 2.1 nm (top), 2.5 nm (bottom). Parameters: top, V_{tip}100 mV, setpoint 59 pA; bottom, V_{tip} 200 mV, setpoint 150 pA.

nm thick films with scan size 50 nm are shown in Figs. 1–3. It is clear that as the growth temperature is increased, the islands both increase in size and become squarer. Table I gives the average island diameter and the overall roughness averaged over several 200 nm images.

The difference caused by increasing the growth temperature from 80 to 295 K is mainly a small increase in island size, together with an increase in roughness (Fig. 1). The islands also appear to become less rounded, and less uniform in size. It should be noted that the lower temperature sample was annealed to room temperature before measuring, and definite changes in the LEED pattern were observed. A much more dramatic change is observed as the growth temperature is increased to 395 K (Fig. 2). The islands begin to become square, with a decrease in roughness being observed.

Between 395 and 495 K a subtle change occurs in the island shape. At the lower temperature, round structures within the islands are still visible, but at the higher temperature, the structure changes to square pyramidal islands with clearly defined steps on their faces. At this point the increased step edge diffusion has begun to dominate, causing square islands.

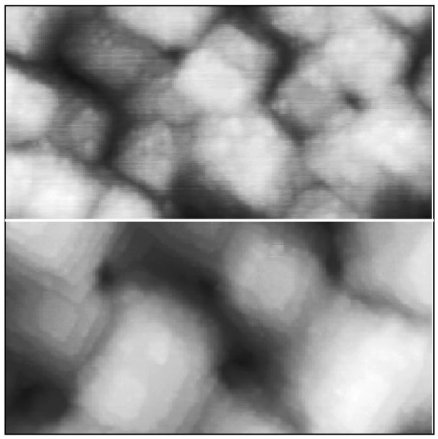

FIG. 2. STM images for growth at 395 (top) and 495 (bottom). Images 50 ×25 nm. Both images have a black-white height of 2.1 nm. Parameters: top, V_{tip}250 mV, setpoint 190 pA; bottom, V_{tip}140 mV, setpoint 235 pA.

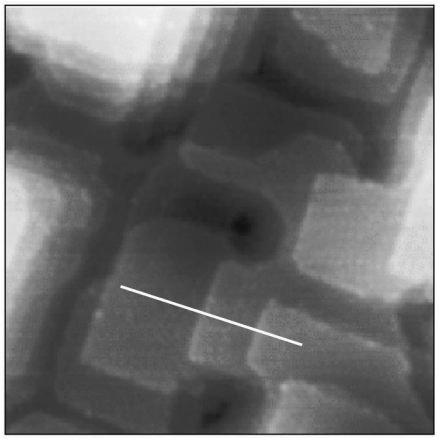

FIG. 3. 50×50 nm STM image for growth at 595 K. Black-white contrast 0.9 nm. Parameters: V_{tip}—86 mV, setpoint 90 pA.

Several authors have reported pyramid growth of Fe on MgO[7] at a temperature of 400–450 K and GaAs.[14] They found pyramids with facet angles of 27° and 13° respectively, the formation of which was explained in terms of surface diffusion. For a deposition temperature of 395 K we obtained pyramidal islands with facet angles of ≈20°; films grown at higher temperature had much reduced facet angles with clearer atomic steps.

At the highest growth temperature at which continuous films are produced, 595 K, large (>15 nm) terraces are formed. The step edges are aligned along Fe[100]. Two atomic steps are visible along the white line in Fig. 3, with heights corresponding to $a/2$. These large flat terraces may form a basis for further study, such as scanning tunneling spectroscopy; we conclude that this temperature is the optimum to produce flat films, since still higher temperatures produce discontinuous films.

V. MAGNETIC BEHAVIOR

A. Hysteresis

After STM investigation the films were assessed for magnetic properties by *in situ* MOKE. Hysteresis loops were taken with **H** at various angles to the substrate lattice directions. The incident light was *p* polarized, so that the magnetooptic signal was due solely to magnetization in the longitudinal direction,[15] which was parallel to **H**.

A typical hysteresis loop with **H** applied along the magnetic easy axis is shown in Fig. 4(a). The low coercivity and

TABLE I. Average island size and rms roughness summarized. The standard deviation in island sizes was approximately 15% in all cases.

Growth temp.	Average island size (nm)	rms roughness (nm)
80	5.0	0.37
295	7.4	0.52
395	9.1	0.42
495	15.5	0.58
595	30.7	0.28

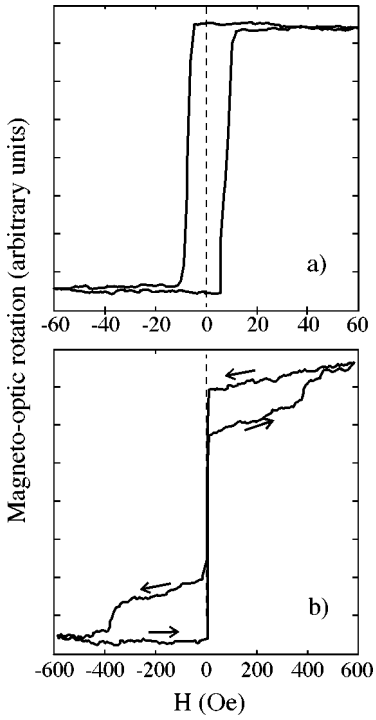

FIG. 4. *In situ* MOKE hysteresis loops from a 5 nm Fe film grown at 295 K. (a) is with **H** along Fe[100], (b) with **H** almost along the magnetic hard axis (Fe[110]).

the steepness of the reversals at the coercive points indicate a high quality epitaxial film with a low concentration of inclusions or defects.

Figure 4(b) shows a typical loop along the magnetic hard axis, which was found to lie along Fe[110]. The secondary jumps seen at ± 400 Oe in Fig. 4(b) are a consequence of the biaxial magnetic anisotropy; similar loops have been reported by Postava *et al.*[16] in Fe/MgO and Daboo *et al.*[17] in Fe/GaAs. All films with growth temperatures at or below 595 K showed this behavior.

The processes governing the presence of the jumps mentioned in the paragraph above are explained in Fig. 5. The diagram shows the evolution of the magnetization, **M**, for a small positive **H**, just before the coercive point is reached. If $\theta = \pi/4$, then the two directions I and I' will both be equivalent. The transitions $I \rightarrow A$ and $I' \rightarrow B$ are energetically equivalent, hence at the coercive point ($\mathbf{H} > 0$) A and B are both equally likely as final destinations for **M**. Experimentally, we found that when **H** is applied *exactly* along either

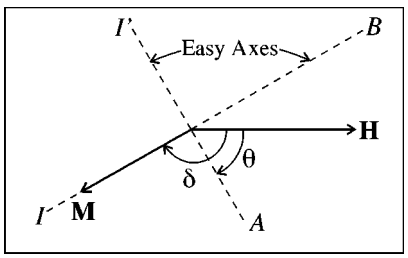

FIG. 5. Magnetization processes in a biaxial film. As **H** increases from negative saturation, **M** will move from I to A. A further jump can then occur when **M** moves from A to B for certain values of θ.

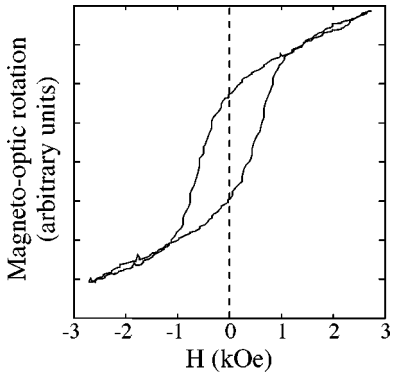

FIG. 6. *Ex situ* MOKE loop for a 10 nm Fe film protected by 2 nm of Au grown at 695 K.

hard axis, then no secondary steps in the hysteresis loop are seen. We believe that this is due to domain formation, the hysteresis behavior being then due to domain motion, rather than abrupt changes of magnetization. Alternatively, the steps may have moved to a field greater than 600 Oe, the maximum field attainable.

If θ is slightly greater than $\pi/4$, then **M** will lie initially along I, since this easy axis is closer to negative **H**. Easy axis A will become slightly preferable over B at positive **H**, since **M** will have to turn through a smaller distance to reach it from the initial state, I. However, **M** will eventually lie along B since A is further from **H**. The motion of **M** from A to B causes the secondary jumps seen in Fig. 4(b). Gu *et al.*[18] have investigated this process by Lorentz microscopy and determined that this jump occurs by domain motion. Measurements of the hysteresis loops support the assertion that **M** in Fig. 4(b) lies along A between 10 and 400 Oe. Experimentally, the position, but not the height of the steps is found to depend strongly on θ.

A uniaxial anisotropy revealed in the hysteresis loop taken along a particular easy axis has been reported by Postava *et al.*[16] and Durand *et al.*[3] The loops displayed steps where the longitudinal magnetization was zero between 0 and approximately 10 Oe. The loops were perfectly symmetrical. We also saw steps between 7 and 10 Oe in our hysteresis loops when **H** was applied within 20° of *either* easy axis in our case. The loops were asymmetric, with the step appearing only on one side of the loop. The longitudinal magnetization at the steps was also nonzero. We believe that our steps are due to domain motion rather than switching processes due to an inequivalence of the magnetic easy axes.

Figure 6 shows a hysteresis loop from a film grown at 695 K, at which the films become discontinuous. This shape is characteristic of a particulate system. The sample displayed no magnetic anisotropy. Paramagnetic behavior has also been reported by Park *et al.*[19] at growth temperatures of 700 K.

B. Determination of K_1/M

A second series of samples was grown for the *ex situ* determination of the ratio of the first cubic magnetic anisotropy parameter K_1 [see Eq. (1)] to the saturation magnetization, M. The samples were 10 nm thick (to provide a larger

TABLE II. Summary of the values of K_1/M (in Oe) for 10 nm Fe films protected by 2 nm Au at various temperatures.

Au growth temp. (K)	80	160	295	595
Fe growth temp. (K)				
80	216±10			
160		225±6		
295			232±8	
383			232±8	
595	190±6		208±8	190±6

magnetooptic signal), protected from oxidation by 2 nm of Au. The growth temperatures of the layers were varied independently to isolate effects due to increased interdiffusion between the Au and Fe; the temperatures and measured values of K_1/M are summarized in Table II.

The amount of interdiffusion between the Au and Fe layers was assessed by AES of the completed sample. Typically, the Fe peak due to the underlayer was 4% of the height of the Au (overlayer) peak. Little correlation of this ratio with growth temperature was seen; however it increased to 30% when the Au layer was grown at 595 K, indicating significant intermixing.

The technique used relies on measuring hysteresis loops magnetooptically as the sample is rotated in-plane. Use of vectorial MOKE[15,20] allows the components of **M** normal (but in-plane) and parallel to the applied field, **H**, to be measured independently. The angle δ between **M** and **H** can then be found, and plotted against the in-plane angle, θ (see Fig. 5). This yields similar information to that produced by a torque magnetometer,[21] and is used to determine K_1. Typical δ versus θ curves are shown in Fig. 7, together with simulations found by minimizing the free energy equation,[22] which consists of an anisotropy and a magnetostatic term,

$$E=-\frac{K_1}{8}\cos 4(\delta-\theta)-MH\cos\delta \quad \text{(c.g.s. units assumed)}. \quad (1)$$

In practice, 8 curves with H ranging between 50 and 3000 Oe were measured. The curves show the expected behavior for a biaxial system — no evidence of uniaxial anisotropy was seen at these fields.

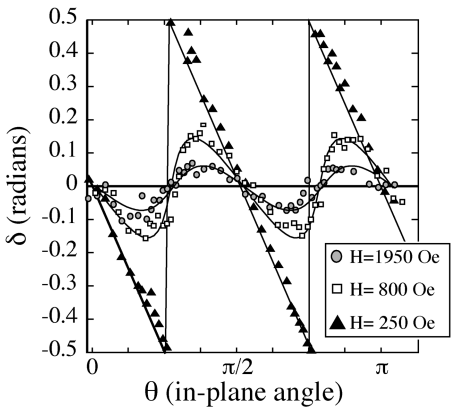

FIG. 7. Curves showing δ (angle between **H** and **M**) as a function of θ (in-plane angle) for several values of H. The biaxial anisotropy is clearly seen. The solid lines are simulations, the points experimental values.

The values of K_1/M were found from the δ versus θ curves by making a discrete Fourier transform of the values of $\sin\delta$ as described by Pastor and Torres,[23] whose equations are equally applicable to biaxial anisotropy if their periodicities are doubled. The component with a periodicity of 4π in data over the range $0\leqslant\theta<\pi$ is given by

$$f_{4\pi}=\frac{N}{2}[H_k/H-\tfrac{1}{2}(H_k/H)^3], \quad (2)$$

where N is the number of data points and H_k is $K_1/2M$. Here, $H_k/H\leqslant\frac{1}{2}$. Analysis of the $\delta-\theta$ curves yields the relation between $f_{4\pi}$ and H, which can then be fitted to Eq. (2) to give H_k. The quality of fit was used to estimate the error in H_k. Tests performed on using data from numerical solutions of Eq. (1) demonstrated the correctness of this method.

The values of K_1/M are all equal within experimental error, indicating that the effect of varying the deposition temperature on the magnetic anisotropy is too small for this technique to measure. One sample was grown with the Fe flux incident along the Fe[100] directions. This gave a H_k value of 148±10, scant evidence that the direction of incident atoms relative to the substrate lattice affects the biaxial anisotropy. We could not detect any difference in the hysteresis loops from this sample and one grown at the same temperature with the Fe flux along Fe[110]. The values with flux along Fe[110] are quite close to the bulk value, which lies between 260 and 280 Oe.[24]

Vibrating sample magnetometer (VSM) measurements gave the saturation magnetization of the films to be 1800 ±200 emu/cc, consistent with the bulk value. Our technique was not sensitive enough to make any difference between the samples apparent, however.

Goryunov *et al.*[25] measured K_1/M over a wide range of thicknesses at various temperatures. They found that this parameter varies strongly with film thickness, the difference at low thicknesses also depending on temperature. The values at 300 and 475 K were 185 and 236 Oe respectively for a 10 nm sputtered film. Kohmoto and Alexander[12] reported a value of 300 Oe for an epitaxial film.

VI. CONCLUSIONS

We have found an interesting relation between island shape and size with growth temperatures between 80 and 595 K; at still higher temperatures the Fe became particulate. This forms a useful system, since rough, smooth or discontinuous oriented films can be chosen simply by selection of the deposition temperature. However, the magnetic properties of the Fe appear to be fixed within the epitaxial temperature range.

It is possible that a change in magnetic anisotropy with growth temperature occurs, since it has been reported that the lattice parameter of Fe has a complex thickness dependence with the most pronounced changes around 10 monolayers.[8] A change in deposition temperature will affect the Fe/MgO interface, and perhaps also the lattice parameter and magnetic properties of a thin film. However, our films were much thicker than this in order to provide sufficient magnetooptic signal. This perhaps explains our failure to find a correlation

of the value of K_1/M with deposition temperature. The effect of the step edges on K_1 is likely to be small, since their effect is inversely proportional to film thickness.[14] Atomic steps on the substrate surface have been shown to affect the anisotropy of a film,[26] but only at a deposited thickness equivalent to 2 monolayers. The use of thinner films will increase the perturbing effects of the Au capping layer, necessitating the use of *in situ* MOKE for anisotropy measurements. This is made difficult by the high H field required.

ACKNOWLEDGMENTS

The work here has been financially supported by the Dutch Foundation for the Fundamental Research of Matter (FOM), which is, in turn, financially supported by the Dutch Organization for Scientific Research (NWO). One of the authors (J.F.L.) would like to acknowledge the assistance of the Human Capital and Mobility program of the European Community (Contract No. ERBCHBICT 94 1207). R.S. would like to acknowledge the assistance of the Brite-Euram program of the European Community (contract number BRE 2-CT93-0569). The help of A. M. Keen is also acknowledged.

[1] C. Li and A. Freeman, Phys. Rev. B **43**, 780 (1991).
[2] Y. Park, E. Fullerton, and S. Bader, Appl. Phys. Lett. **66**, 2140 (1995).
[3] O. Durand, J. Childress, P. Galtier, R. Bisaro, and A. Schulhl, J. Magn. Magn. Mater. **145**, 111 (1995).
[4] J. Stroscio, D. Pierce, A. Davies, R. Celotta, and M. Weinert, Phys. Rev. Lett. **75**, 2960 (1995).
[5] Y. Huang, C. Liu, and G. Felcher, Phys. Rev. B **47**, 183 (1992).
[6] R. Schwoebel, J. Appl. Phys. **40**, 614 (1969).
[7] K. Thürmer, R. Koch, M. Weber, and K. Rieder, Phys. Rev. Lett. **75**, 1767 (1995).
[8] B. Lairson, A. Payne, S. Brennan, N. Rensing, B. Daniels, and B. Clemens, J. Appl. Phys. **78**, 4449 (1995).
[9] T. Urano and T. Kanaji, J. Phys. Soc. Jpn. **57**, 3403 (1988).
[10] J. Lawler, R. Schad, S. Jordan, and H. van Kempen, J. Magn. Magn. Mater. **165**, 224 (1997).
[11] P. Thibado, E. Kneedler, B. Jonker, B. Bennett, B. Schanabrook, and L. Whitman, Phys. Rev. B **53**, R10481 (1996).
[12] O. Kohmoto and C. Alexander, Jpn. J. Appl. Phys., Part 1 **31**, 2101 (1992).
[13] H. Ohta, S. Imagawa, M. Motokawa, and E. Kita, J. Phys. Soc. Jpn. **62**, 4467 (1993).
[14] M. Gester, C. Daboo, S. Gray, and J. Bland, J. Magn. Magn. Mater. **165**, 242 (1997).
[15] S. Jordan and J. Whiting, Rev. Sci. Instrum. **67**, 4286 (1996).
[16] K. Postava, H. Jaffres, F. Nguyan van Dau, M. Goiran, and A. Fert, J. Magn. Magn. Mater. **172**, 199 (1997).
[17] C. Daboo, R. Hicken, D. Eley, M. Gester, S. Gray, A. Ives, and J. Bland, J. Appl. Phys. **75**, 5586 (1994).
[18] E. Gu, J. Bland, C. Daboo, M. Gester, L. Brown, R. Ploessl, and J. Chapman, Phys. Rev. B **51**, 3596 (1995).
[19] Y. Park, S. Adenwalla, G. Felcher, and S. Bader, Phys. Rev. B **52**, 12779 (1995).
[20] C. Daboo, J. Bland, R. Hicken, A. Ives, M. Baird, and M. Walker, Phys. Rev. B **47**, 11852 (1993).
[21] S. Jordan and C. Prados, J. Magn. Magn. Mater. **172**, 69 (1997).
[22] R. Bozorth, Phys. Rev. **50**, 1076 (1936).
[23] G. Pastor and M. Torres, J. Appl. Phys. **58**, 920 (1985).
[24] *Magnetic Properties of Metals, d-elements, Alloys and Compounds, Data in Science and Technology*, edited by H. Wijn (Springer, Berlin, 1991).
[25] Y. Goryunov, N. Garifyanov, G. Khaliunnin, I. Garifullin, L. Tagirov, F. Schreiber, T. Muhge, and H. Zabel, Phys. Rev. B **52**, 13450 (1995).
[26] D. Huang, J. Lee, G. Mulhollan, and J. Erskine, J. Appl. Phys. **73**, 6751 (1993).